Indian J. Phys. 74B (4), 281–286 (2000)

I J P B
— an international journal

Free space reflection type microwave interferometric method for dielectric studies of sheet materials

R K Khanna* and S K Upadhyay

Microwave and Plasma Laboratory, Department of Physics, Government College, Ajmer-305 001, India

Received 10 November 1999, accepted 10 May 2000

Abstract : A system is described for measuring the complex permittivity of dielectric sheet materials in the X-band of microwave frequencies at 9.28 GHz using free space normal reflection technique. It is a non-destructive type method which involves multiple reflections inside the specimen. First order analysis is presented for the effect of multiple reflection in thick low-loss dielectric sheets under conditions of oblique incidence. Values of ε' and ε'' are given for Paper and overhead projector Transparency sheets at room temperature that are estimated to be accurate to ± 0.5%

Keywords Microwave technique, dielectric measurements, interferometer

PACS Nos. : 07.60 Ly, 77.22.Ch, 84.40.Az

1. Introduction

Measurement of dielectric properties of medium and low lossy samples in the microwave region are often performed by analyzing the profile of the power reflected from a cell of standard rectangular waveguide filled with dielectric and terminated by shorting plunger [1–5]. As discussed in a survey paper by Lynch [6] on such measurement techniques, the problem is to find a sample of proper configuration which on insertion in dielectric cell produces a precise calculable effect on reflection profile. Careful preparation of sample dimension is must for these methods which produces variety of problems and sources of error. For certain industrial materials such as glass, plastic *etc.* which cannot easily be machined, these methods are of limited use. Most of the dielectric materials employed in industry or otherwise are in the form of sheets, strips or thin films. In such forms, *r.f.* signal has a weak interaction with the sample and therefore conventional methods for dielectric studies, which are based on the measurement of attenuation and phase shift caused by the sample in the *r.f.* field are not expected to give very accurate results [7–9].

This paper describes a free space reflection type interferometric technique for the measurement of dielectric parameters of the dielectric sheet materials in the X-band of microwaves. This is non-destructive type method where sample interact with microwaves in free space and works on the principle of multiple wave interference in thick dielectric sample. Details of waveguide transmission and detecting systems employed in a modified Febry-Perot type interferometer configuration are presented here. Theory of the experimental method along with the curve fitting technique and data analysis for evaluation of dielectric parameters *etc.* are described below at some length. Results of dielectric constant and loss factor are given for selected materials at 9.28 GHz and 32°C.

2. Theory of the experimental method

The working of reflection type interferometer is based on multiple wave interference theory [10,11]. Microwave beam SR_0 incident upon the air-dielectric interface at an angle ϕ gives rise to an infinite number of parallel transmitted rays T_1T_1', T_2T_2', T_3T_3' *etc.* and parallel reflected rays R_0R_0', R_1R_1', R_2R_2' *etc.* as shown Figure 1. The phase difference between two neighbouring reflected rays from the source to the receiver is represented by the relation

$$\nabla = \frac{2\pi}{\lambda_0}\left[\frac{2nZ}{\cos\phi'} + \frac{2n'Z'}{\cos\theta'} - 2nZ'\tan\theta'\sin\phi - 2nz\tan\phi'\sin\phi\right] \qquad (1)$$

here n & n' are the refractive indices and Z & Z' are the thickness of the dielectric sample and glass plate respectively. ϕ and ϕ' are the angle of incidence and angle of refraction at air-dielectric interface while θ' is the angle of refraction at dielectric-glass interface.

*For correspondence

For normal incidence

$$\phi = \phi' = \theta' = 0 .$$

Therefore eq. (1) becomes

$$\nabla = \frac{2\pi}{\lambda_0}(2nZ + 2n'Z'),$$

$$\nabla = \frac{2\pi}{\lambda_d} 2Z + \frac{2\pi}{\lambda_g} 2Z'$$

$$= 2\beta Z + 2\beta' Z'$$

$$= 2\beta Z + 2\delta' , \qquad (2)$$

where γ_0, γ_d and γ_g are the wavelengths of microwave in free space, in dielectric sample and in glass respectively. β and β' are the phase shift constants due to dielectric sample and glass plate respectively. Here, $\delta' = \beta' Z'$ is a constant as the thickness of the glass plate (Z') remains same during the measurements. In the theoretical treatment of interferometer, following symbols are used :

T = Ratio of the transmitted to the incident amplitude when the wave passes from the glass plate to the free space (air).

T' = Ratio of the transmitted to the incident amplitude when the wave passes from the free space (air) to the dielectric specimen.

R = Ratio of the reflected to the incident amplitude when the wave passes from the glass plate to the free space.

R' = Ratio of the reflected to the incident amplitude when the wave passes from the free space to the dielectric specimen.

τ = Ratio of the transmitted to the incident amplitude when the wave passes from the dielectric specimen to the glass plate.

τ' . Ratio of the transmitted to the incident amplitude when the wave passes from the glass plate to the dielectric specimen.

t' = Ratio of the transmitted to the incident amplitude when the wave passes from the dielectric specimen to the free space.

r = Ratio of the reflected to the incident amplitude when the wave passes from dielectric specimen to the free space.

The first ray $R_0 R_0'$ is reflected from the air-dielectric interface UU' and does not enter inside the dielectric. Second ray $R_1 R_1'$ has undergone four refractions and one internal reflection (see Figure 1) and has travelled a distance $2Z$ (for normal incidence) inside the dielectric sample. Therefore, it will be attenuated by a factor exp $(-\alpha.2Z)$ where α is the attenuation coefficient in neper/cm. associated with the dielectric for incident microwave beam. The reflections at dielectric-glass interface are going to be small according to Fresnel's equations and have been neglected to avoid the mathematical complexity. The third reflected ray $R_2 R_2'$ has

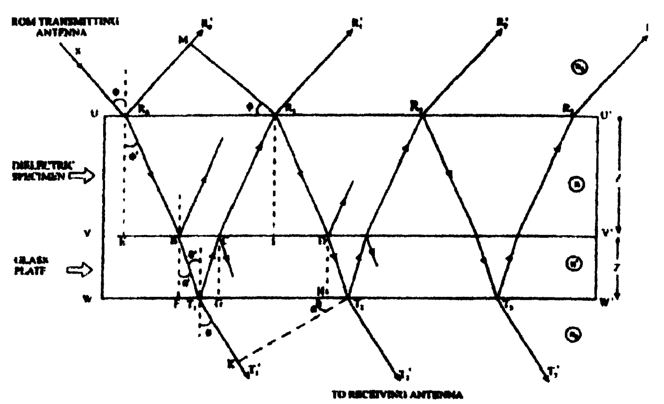

Figure 1. Ray diagram of multiple wave interference.

undergone six refractions and three times internal reflections and has travelled a distance equal to $4Z$ (for normal incidence) inside the sample. Therefore, it will be attenuated by a factor exp $(-\alpha.4Z)$ and so on for the other successive rays. If E_{r0}, E_{r1}, E_{r2}, E_{rm} *etc.* are the amplitudes of the electric field vectors of the first, second, third and m-th ray successively then these can be expressed as :

$$E_{r0} = R' E_0 e^{j\omega t},$$

$$E_{r1} = T't'\tau\tau' R E_0 e^{j\omega t} e^{-j\nabla} e^{-\alpha.2Z},$$

$$E_{r2} = T't'\tau^2\tau'^2 R^2 r E_0 e^{j\omega t} e^{-j2\nabla} e^{-\alpha.4Z}$$

$$E_{rm} = T't'\tau^m\tau'^m R^m r^{(m-1)} E_0 e^{j\omega t} e^{-jm\nabla} e^{-\alpha.2mZ}$$

$$= T't'\tau\tau' R E_0 e^{j\omega t} e^{-j\nabla} e^{-2\alpha Z}\left[\tau\tau' R r e^{-j\nabla} e^{-2\alpha Z}\right]^{(m-1)} .$$

Let E_r be the resultant amplitude of the electric field vector of the reflected wave, then using the principle of superposition it can be expressed as

$$E_r = E_{r0} + E_{r1} + E_{r2} + \cdots + E_{rm} + \cdots$$

$$= E_0 e^{j\omega t}\Big[R' + T't'\tau\tau' \mathrm{R} e^{-2\alpha Z} \times \sum_{m=1}^{\infty}\left(\tau\tau' R r e^{-j\nabla} e^{-2\alpha Z}\right)^{(m-1)}\Big]$$

The infinite sum $\sum_{m=1}^{\infty}\left(\tau\tau' R r e^{-j\nabla} e^{-2\alpha Z}\right)^{(m-1)}$ is equal to $\left(\frac{1}{1 - \tau\tau' R r e^{-j\nabla} e^{-2\alpha Z}}\right)$ therefore,

$$E_r = E_0 e^{j\omega t}\left[\frac{R' - \tau\tau' R R' r e^{-j\nabla} e^{-2\alpha Z} + T't'\tau\tau' \mathrm{R} e^{-j\nabla} e^{-2\alpha Z}}{1 - \tau\tau' R r e^{-j\nabla} e^{-2\alpha Z}}\right].$$

If P_r is the power of reflected wave then it can be expressed as

$$P_r = E_r . E_r^* ,$$

where E_r^* is the complex conjugate of E_r.

Thus $P_r = P_i R'^2$

$$\frac{\left\{1+\frac{\tau\tau' R}{R'}(T't'-R'r)e^{-2\alpha Z}\right\}^2 - \frac{4\tau\tau' R}{R'}(T't'-R'r)e^{-2\alpha Z}\sin^2\frac{\nabla}{2}}{(1-\tau\tau' Rre^{-2\alpha Z})^2 + 4\tau\tau' Rre^{-2\alpha z}\sin^2\frac{\nabla}{2}} \tag{3}$$

here $P_i = E_0^2$ is the power of incident microwave beam. The complex dielectric constant of a dissipative dielectric media is represented by $\varepsilon^* = \varepsilon' - j\varepsilon''$ where

$$\varepsilon' = \left(\frac{\lambda_0}{\lambda_d}\right)^2 \left[1 - \frac{\alpha^2}{\beta^2}\right] \text{ and } \varepsilon'' = \left(\frac{\lambda_0}{\lambda_d}\right)^2 \frac{2\alpha}{\beta}; \tag{4}$$

we know that, ε^* can also be expressed as

$$\varepsilon^* = \varepsilon'(1 - j\tan\delta),$$

where dimensionless quantity $\delta = \varepsilon''/\varepsilon'$ is called loss tangent.

3. Details of the experimental set up

Reflection type interferometer for the measurement of dielectric parameters of materials in the form of sheets has been assembled on a specially designed wooden bench. The block diagram of the experimental set up is shown in Figure 2. Microwave power generated by reflex Klystron (2K25) was fed into the pyramidal horn antenna through an

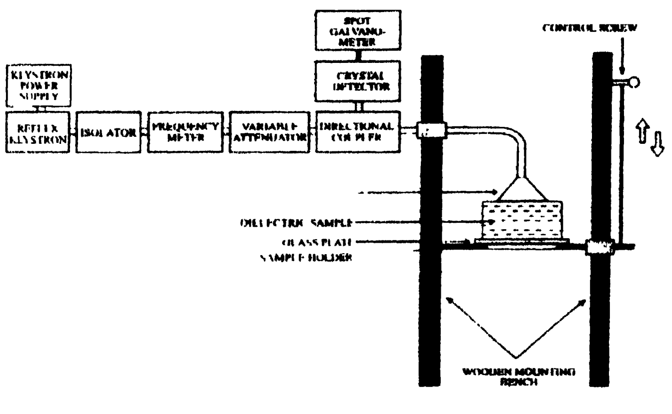

Figure 2. Schematic of microwave reflection type interferometric set-up

isolator, frequency mater, variable attenuator and a directional coupler. The same horn antenna was used as transmitter as well as receiver for the microwave beam incident on or reflected from the dielectric sample. The microwave power reflected by the dielectric sample was detected and measured by the microwave crystal detector connected at fourth port of the directional coupler. Reflected power was observed in divisions of spot galvanometer, which was attached to the detector by a coaxial wire. Microwave power transmitted from the antenna was controlled by variable anttenuator and its frequency was determined by frequency meter. Samples under study were placed on a specially made glass plate. The glass plate was kept on a specially designed sample holder whose position could be varied vertically and measured with an accuracy of 1 mm.

Some parts of the apparatus were fixed on a skilfully designed wood bench of 2 meters height. Provisions were made in this bench to level the sample holder along with the glass plate so that microwave beam would fall normally on the sample.

4. Procedure for the measurement of reflection profile

Klystron was switched on about half an hour before the actual measurements were taken for the power and frequency stability. Glass plate was placed on the sample holder and the sample sheets were placed on the glass plate. The horn antenna was adjusted in such a way that upper surface of the sample could just touch the horn antenna. Sample thickness (Z) was varied by putting a bunch of ten sheets each time on the glass plate and the corresponding reflected power (P_r) was recorded in number of divisions of spot galvanometer. The thickness of ten sheets of Paper and overhead projector Transparencies were 0.103 cm and 0.1 cm respectively. Therefore, the thickness (Z) of Paper sheets was increased in the steps of 0.103 cm and that of Transparency sheets in the steps of 0.1 cm. About 70 observations were taken for each sample. Operating frequency of Klystron was 9.28 GHz corresponding to free space wave length, $\lambda_0 = 3.232$ cm. The typical variation of P_r with Z for Paper sheets is shown in Figure 3.

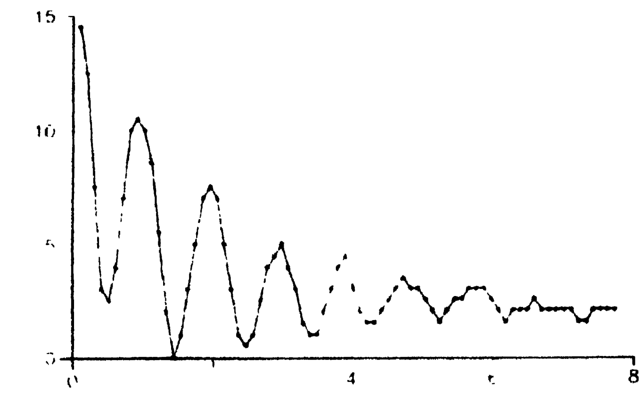

Figure 3. Typical variation of reflected power (P_r) with sample thickness (Z) for Paper sheet.

5. Method of determining dielectric parameters

To determine the dielectric parameters, the values of α, β, λ_d and λ_0 were evaluated. First, the approximate value of attenuation coefficient was determined and then using computer for curve fitting, accurate value of α is estimated.

5.1. Determination of approximate value of anttenuation coefficient :

From eq. (3) it follows that, P_r will be maximum when $\sin^2(\beta Z + \delta')$ will be maximum *i.e.* $\sin^2(\beta Z + \delta') =$. By substituting this value in eq. (3), the maximum value of reflected power, say $(P_r)_{Max}$ would be

$$(P_r)_{Max} = P_i R'^2 \frac{1 - \frac{\tau\tau' R}{R'}(T't' - R'r)e^{-2\alpha Z_{Max}}}{1 + \tau\tau' R r e^{-2\alpha Z_{Max}}} \quad . \quad (5)$$

Similarly, the minimum value of reflected power would be

$$(P_r)_{Min} = P_i R'^2 \frac{1 - \frac{\tau\tau' R}{R'}(T't' - R'r)e^{-2\alpha Z_{Min}}}{1 + \tau\tau' R r e^{-2\alpha Z_{Min}}} \quad . \quad (6)$$

Here, Z_{Max} and Z_{Min} are the thickness of dielectric sample corresponding to $(P_r)_{Max}$ and $(P_r)_{Min}$ respectively.

By taking logarithm on both sides of eq. (5) one gets

$$\ln(P_r)_{Max} = \ln\left(P_i R'^2\right) + 2\ln\left[1 - \frac{\tau\tau' R}{R'}(T't' - R'r)e^{-2\alpha Z_{Max}}\right]$$

$$-2\ln\left[1 + \tau\tau' R r e^{-2\alpha Z_{Max}}\right]. \quad (7)$$

Electromagnetic wave suffers a phase change of π radian when reflected from the denser medium and hence R and R' are of opposite sign. Hence taking $\frac{\tau\tau' R}{R'}(T't' - R'r)$ to be a negative quantity, eq. (7) can be rewritten as

$$\ln(P_r)_{Max} = \ln\left(P_i R'^2\right) + 2\ln\left[1 + \frac{\tau\tau' R}{R'}(T't' - R'r)e^{-2\alpha Z_{Max}}\right]$$

$$-2\ln\left[1 + \tau\tau' R r e^{-2\alpha Z_{Max}}\right]. \quad (8)$$

One knows that for small value of x

$$\left.\begin{aligned} \ln(1 - x) &= -x \\ \text{and} \quad \ln(1 + x) &= x. \end{aligned}\right\} \quad (9)$$

Since the values of $\frac{\tau\tau' R}{R'}(T't' - R'r)e^{-2\alpha Z_{Max}}$ and $\tau\tau' R r e^{-2\alpha Z_{Max}}$ will be small, eq. (8) (using eq. (9)) can be expressed as

$$\ln(P_r)_{Max} = \ln\left(P_i R'^2\right) + 2\left[\frac{\tau\tau' R}{R'}(T't' - R'r)e^{2\alpha Z_{Max}}\right]$$

$$-2\left[\tau\tau' R r e^{-2\alpha Z_{Max}}\right]$$

$$= \ln\left(P_i R'^2\right) + 2e^{-2\alpha Z_{Max}}\left[\frac{\tau\tau' R T't'}{R'} - 2\tau\tau' R r\right]. \quad (10)$$

By expanding $e^{-2\alpha Z_{Max}}$ in a series and considering the value of $2\alpha Z_{Max}$ to be small and therefore neglecting higher powers of $2\alpha Z_{Max}$, eq. (10) can be written as

$$\ln(P_r)_{Max} = \ln\left(P_i R'^2\right) + 2\left[\frac{\tau\tau' R T't'}{R'} - 2\tau\tau' R r\right]$$

$$\times\left[1 - 2\alpha Z_{Max}\right]$$

$$= \ln\left(P_i R'^2\right) + 2\left[\frac{\tau\tau' R T't'}{R'} - 2\tau\tau' R r\right]$$

$$-4\left(\frac{\tau\tau' R T't'}{R'} - 2\tau\tau' R r\right)\alpha Z_{Max}$$

$$= \left[\ln\left(P_i R'^2\right) + 2\left(\frac{\tau\tau' R T't'}{R'} - 2\tau\tau' R r\right)\right] - X\alpha Z_{Max}, \quad (11)$$

where $x = 4\left(\frac{\tau\tau' R T't'}{R'} - 2\tau\tau' R r\right)$

and $C = \left[\ln\left(P_i R'^2\right) + 2\left[\frac{\tau\tau' R T't'}{R'} - 2\tau\tau' R r\right]\right]$

are the constant quantities. On comparing eq. (11) with standard equation of a straight line, one cane observe that a plot of $\ln(P_r)_{Max}$ *versus* Z_{Max} will be a straight line whose slope will be equal to $-X\alpha$. As an example, the method of determining the dielectric parameters of Paper sheets is given here.

Figure 4 shows the plot of $\ln(P_r)_{Max}$ *versus* Z_{Max} for Paper sheet. This plot is straight line whose slope is -0.264. Therefore, one can write,

$$X\alpha = 0.264.$$

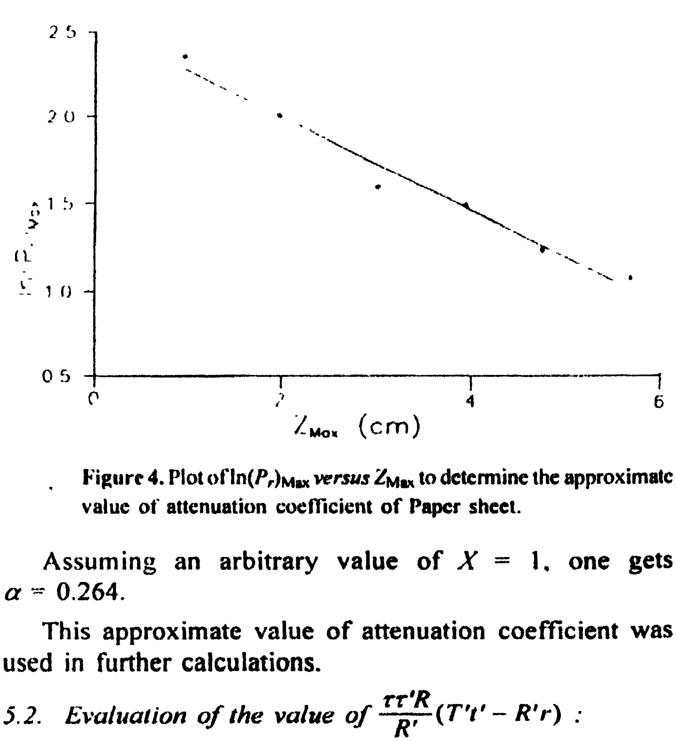

Figure 4. Plot of $\ln(P_r)_{Max}$ *versus* Z_{Max} to determine the approximate value of attenuation coefficient of Paper sheet.

Assuming an arbitrary value of $X = 1$, one gets $\alpha = 0.264$.

This approximate value of attenuation coefficient was used in further calculations.

5.2. Evaluation of the value of $\frac{\tau\tau' R}{R'}(T't' - R'r)$:

From the data of P_r and Z for paper sheet, the maximum and minimum values of P_r *i.e.* $(P_r)_{Max}$ and $(P_r)_{Min}$ corresponding to sample thickness Z_{Max} and Z_{Min} were identified. By substituting the values of Z_{Max}, Z_{Min}, $(P_r)_{Max}$ and $(P_r)_{Min}$ for first maximum and minimum positions, $\alpha = 0.264$ and arbitrary value of $\tau\tau' R r = 0.1$ in eqs. (5) and (6) and then dividing eq. (5) by eq. (6), the value of $\frac{\tau\tau' R}{R'}(T't' - R'r)$ was evaluated. Similarly, the values of $\frac{\tau\tau' R}{R'}(T't' - R'r)$ for other maximum and minimum position were evaluated. The arithmetic mean of all the values of $\frac{\tau\tau' R}{R'}(T't' - R'r)$ is found to be −2.265, in case of Paper sheet.

5.3. Estimation of the value of $P_t R'^2$:

By substituting the values Z_{Max} and $(P_r)_{Max}$ for first maximum position, $\alpha = 0.264$, $\tau\tau' Rr = 0.1$ and $\frac{\tau\tau' R}{R'}(T't' - R'r) = 2.265$ in eq. (5), the value of $P_t R'^2$ was determined. Similarly the values of $P_t R'^2$ were determined for other maximum positions. The arithmetic mean of all the values of $P_t R'^2$ was taken and was found to be 2.455.

5.4 Determination of phase shift constant (β) and additional phase (δ') :

From the observed oscillatory pattern of the curve between P_r and Z (see Figure 3), the value of wavelength in dielectric (λ_d) was obtained. The analysis of the theory of reflection type interferometer indicates that the separation between the successive maxima and minima should be equal to $\lambda_d/2$. For Paper sheets the value of $\lambda_d/2$ was found to be equal to 0.968 cm. Therefore, phase shift constant (β) would be equal to 3.245 cm−1.

From $\sin^2(\beta Z + \delta') =$

$$\delta' = (2N+1)\frac{\pi}{2} - \beta Z_N.$$

Here, Z_N corresponds to the thickness of the dielectric sample for observed N-th maxima. For first maxima δ' was found to be equal to −1.639 deg.

5.5 Theoretical calculation of the values of P_r :

On putting the values of $\alpha = 0.264$ neper/cm, $\tau\tau' Rr = 0.1$, $\frac{\tau\tau' R}{R'}(T't' - R'r) = 2.265$, $P_t R'^2 = 2.455$, $\beta = 3.245\ \text{cm}^{-1}$ and $\delta' = -1.639$ deg. in eq. (3), theoretically calculated values of P_r were determined corresponding to different values of Z from 0.1 cm to 8 cm. Then the curve between theoretically calculated values of P_r and Z (termed as theoretical curve) was plotted and compared with the observed curve plotted between experimentally obtained values of P_r and Z.

5.6. Curve fitting technique for determining the true value of attenuation coefficient :

Using the similar procedure as mentioned in para 5.1 to 5.5, efforts were made to best fit both the theoretical and experimental curves by changing the values of α and $\tau\tau' Rr$ as fitting parameters. A computer programme in BASIC was formed for eq. (3) for generating the theoretical values of P_r corresponding to different values of Z. Both the experimental and theoretical curves were plotted in the computer using GRAPHER software. Figure 5 shows the best fitted curves for $\alpha = 0.227$ neper/cm and $\tau\tau' Rr = 0.005$ for paper sheets. This indicates that the true value of attenuation coefficient of Paper is 0.227 neper/cm. Using

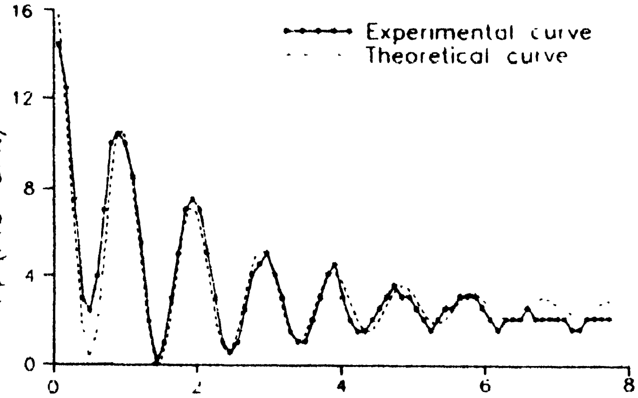

Figure 5. Experimental and theoretical best fitted curves of P_r *versus* Z for Paper sheets.

similar method as mentioned above, the true value of attenuation coefficient of other samples in the form of sheet were determined.

6. Evaluation of ε', ε'' and $\tan\delta$

By putting the values of α (obtained by curve fitting method), β, λ_0 and λ_d in eq. (4), the values of ε' and ε'' for Benzene, Paper and Transparency sheets were determined. Using relation $\tan\delta = \varepsilon''/\varepsilon'$, the loss tangent for different samples were calculated.

7. Results and discussion

The measured values of dielectric parameters for Benzene, Paper and overhead projector Transparency sheets at room temperature (32 ± 3°C) and 9.28 GHz using reflection type interferometric technique are shown in Table 1. This interferometer can be used for the dielectric study of liquids

Table 1. Dielectric parameters of materials at 9.28 GHz and at room temperature (32 ± 3°C)

Dielectric materials	α (neper/cm)	ε'		$\tan\delta$
Paper sheet	0.227	2.77	0.407	0.147
Transparency sheet	0.041	3.39	0.078	0.023
Benzene	0.022	2.26	0.034	0.015

with a small modification *i.e.* glass plate is replaced by a glass tray type cell. Liquid sample is poured into cell is known amount to change the thickness in 1 mm step. Measurements were done on Benzene to test the apparatus and related theory of the technique. Results of Benzene are presented here along with Paper and Transparency sheet. The measured value of dielectric constant of Benzene (2.26) is very near to the reported value (2.29) within 1.32 percent [12]. Benzene used in the present measurement has been obtained from BDH and is of LR grade. Further purification

In the light of above discussions, it becomes necessary to explore into the selection of ideal geometrical parameters of SLG so that the wavelengths may be detected with maximum intensity and maximum efficiency [10]. This may be immensely important in the investigation of biomolecules of the interstellar space.

2. Theory

We have already derived the intensity expression for such a grating elsewhere [11]. The intensity J of the diffracted beam from such a grating, has been calculated by us. It is given by

$$J = 4a^2\left[\frac{\sin\phi}{\phi}\right]^2\left[\frac{\sin^2 4N\phi}{\sin^2 4\phi}\right]$$

$$\left[(2\cos\psi + 1)\cos^2 2\phi + \cos^2\psi\right] \tag{1}$$

$$\text{where } \phi = \pi a \sin\theta \tag{2}$$

$$\text{and} \quad = \frac{2\pi}{\lambda}\left[b(1+\cos\theta) + a\sin\theta\right]. \tag{3}$$

Here, a and b are step size and the height of the steps respectively. N is the number of steps, θ is the diffraction angle and λ is the wavelength of the incident radiation.

We see that J is maximum when sin $(4\phi) = 0$, *i.e.*, when $4a \sin(\theta) = m\lambda$ or $d\theta/d\lambda = m/4a \cos\theta$ (where m is the order of diffraction). It can be easily shown that for all practical purposes, the resolving power is given by the product Nm [12].

The above intensity expression is used to calculate the ideal dimensions of the millimeter wave grating for a particular wavelength as discussed in the next section.

3. Results and discussion

The expression for J can be used for designing mm wave symmetrical lamellar grating for the required wavelength. For example, to find out suitable grating parameters with $N = 30$, at $\lambda = 5$ mm, we can draw a 3D plot of intensity J with the grating parameters a and b as shown in Figure 2. Knowledge of the minimum values of the parameters for optimum response will reduce the construction cost. The parameters for all operating wavelengths can be similarly worked out from the expression for J. The X-band frequency is sometimes used which occurs at 10 GHz. We calculate the antenna beamwidth (θ) as a function of aperture size (l) from 10 GHz through 220 GHz to 300 GHz using the expression [13], $\theta = \frac{4\lambda}{\pi l}$ and represent them in Table 1 and Figure 3.

It is observed from the Table and the Figure that a narrow beamwidth of 0.33° is obtained at one of the propagation windows at 220 GHz for which an aperture size of 30 cm is required. If we want to switch over to other lower frequencies such as 95 GHz, the size of the sperture required will be around 60 cm, *i.e.*, double the size of the former aperture to have a beamwidth of 0.38°. At the frequency of

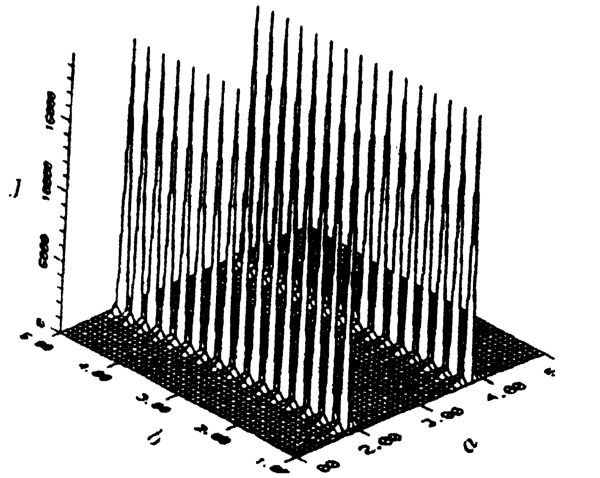

Figure 2. Intensity distribution as a function of the relative thickness a and breadth b of the steps.

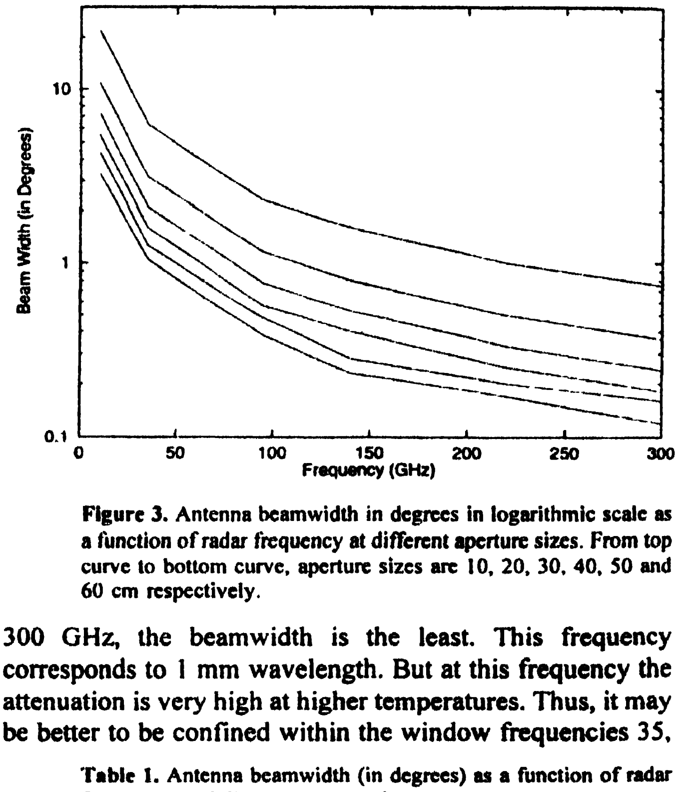

Figure 3. Antenna beamwidth in degrees in logarithmic scale as a function of radar frequency at different aperture sizes. From top curve to bottom curve, aperture sizes are 10, 20, 30, 40, 50 and 60 cm respectively.

300 GHz, the beamwidth is the least. This frequency corresponds to 1 mm wavelength. But at this frequency the attenuation is very high at higher temperatures. Thus, it may be better to be confined within the window frequencies 35,

Table 1. Antenna beamwidth (in degrees) as a function of radar frequency at different aperture sizes.

Sr. No.	Aperture Size (cm.)	Frequency in GHz 10	35	95	140	220	300
1	10	21.90	6.30	2.30	1.60	1.00	0.75
2	20	10.90	3.15	1.15	0.80	0.50	0.36
3	30	7.30	2.10	0.77	0.53	0.33	0.24
4	40	5.50	1.60	0.57	0.40	0.25	0.18
5	50	4.40	1.26	0.48	0.28	0.20	0.16
6	60	3.60	1.05	0.38	0.23	0.17	0.12

95, 140 and 220 GHz where attenuation is minimum. The frequencies roughly correspond to 8.5 mm, 3.0 mm, 2.1 mm and 1.4 mm. A big aperture of 60 cm or more is needed to work at 8.5 mm where the beamwidth is 1.05°. Thus, a mm wave radar provides wide bandwidth which is the largest at 220 GHz.

We now examine the propagation of the mm waves in the presence of cloud and fog at different temperatures. The fog and cloud attenuation properties are depicted in Figure 4 from the experimental data of Kulpa and Brown [13,14].

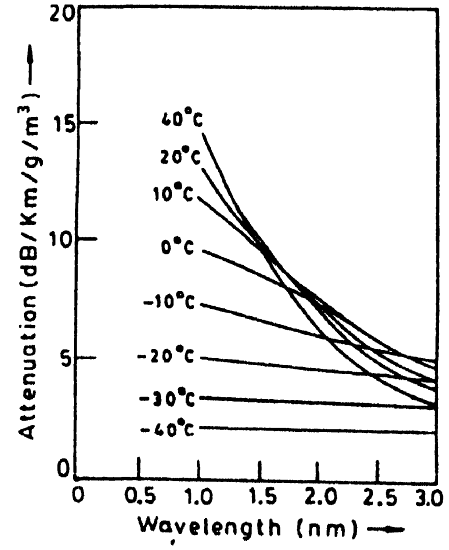

Figure 4. Fog and cloud attenuation properties of millimeter waves

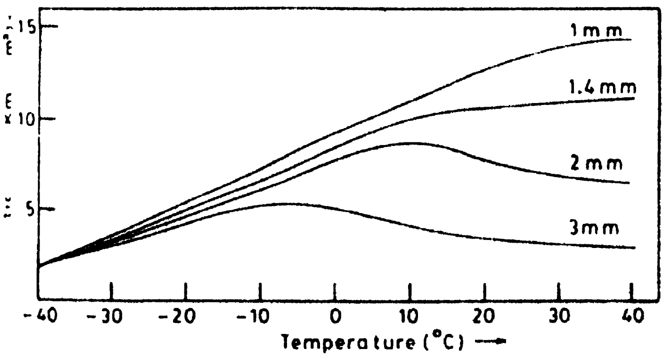

Figure 5. Temperature dependence of attenuation of millimeter waves.

In a tropical country such as India, where the temperature variation is from –20°C (winter in Kashmir) to 45°C (summer in the Delhi belts), it may be worthwhile to study the temperature dependence of fog and cloud attenuation at different wavelengths which we present in Figure 5 using the data of Kulpa and Brown [14].

From Figures 4 and 5, the following characteristics are noted :

1. The attenuation is minimum at ~3 mm (*i.e.* 95 GHz) and above, for all temperatures.
2. At 3 mm wavelength, the attenuation first increases with the rise of temperature and attains a maximum value at – 10°C and gradually decreases to a minimum value. For 2 mm, the maximum however, is attained at 10°C.
3. At –20°C, the attenuation practically remains constant over the entire mm range. At still lower temperatures –30°C and –40°C, the attenuation decreases, but remains the same for all values of mm waves.

These studies on diffraction grating antenna is expected to be useful to detect biomolecules such as glycine, alanine, adenine *etc.* in the interstellar space. As has already been mentioned, these important biomolecules have many of their rotation-vibrational lines in the wavelenth range of 1 to 10 mm.

Acknowledgments

SC thanks Maharaja Manindra Chandra College for cooperation and Centre for Space Physics for technical facilities.

References

[1] Sonali Chakrabarti, K Goswami and J N Chakravorty *Physics Teacher* **39** 35 (1997)

[2] F K Schwering and A A Oliner *Millimeter Wave Antennas in Hand Book Microwave and Optical Components*. ed Kai Chang Vol. I (New York : John Wiley) (1989)

[3] P Khastgir, J N Chakravorty and K K Dey *Indian J Radio Space Phys.* **2** 47 (1973)

[4] K K Dey and P Khastgir *Int J. Electronics* **35** 97 (1973)

[5] K K Dey and P Khastgir *Int. J. Electronics* **36** 91 (1974)

[6] S T Peng, T Tamir and H L Bertoni *IEEE Trans. Microwave Theory Tech.* **MTT-23** 123 (1975)

[7] F Combes, N Q Rieu and G Wlodarczak *Astron Astrophys.* **308** 618 (1996)

[8] S K Chakrabarti and Sonali Chakrabarti *Indian J. Phys* **74B** 97 (2000)

[9] Sonali Chakrabarti and S K Chakrabarti *Astron. Astrophys Lett* **354** L6 (2000)

[10] Sonali Chakrabarti and J N Chakravorty *Opt Commun* **107** 184 (1994)

[11] Sonali Chakrabarti and J N Chakravorty *Astrophys Space Sci.* **209** 99 (1993)

[12] Sonali Chakrabarti *PhD (Sc.) Thesis* (Jadavpur University, India) (1996)

[13] S M Kulpa and E A Brown *HDL-SR-79-8* (1, Harry Diamond Lab, Washington, D.C.) (1979)

[14] *Infrared and Millimeter Waves Vol. 4, Millimeter Systems* eds. Kenneth J Buttom and James C Wiltse (New York : Academic) (1981)